Asian Journal of Control, Vol. 00, No. 0, pp. 1–8, Month 2012
Published online in Wiley InterScience (www.interscience.wiley.com) DOI: 10.1002/asjc.0000

A SECOND ORDER SLIDING MODE PATH FOLLOWING CONTROL FOR AUTONOMOUS SURFACE VESSELS

F. Valenciaga

ABSTRACT

This paper presents a path following control design for an autonomous surface vessel. The considered boat presents three degrees of freedom being driven by two independent propellers placed at its stern and is represented by a highly nonlinear underactuated dynamic model. The control objective is to reach and closely follow a pre-specified trajectory, operating in an environment perturbed by currents and waves. This objective is achieved through a control scheme based on the interaction of guidance laws synthesized by Lyapunov techniques and a high order sliding mode control approach based on the Super Twisting Algorithm. This methodology allows designing robust and simple controllers avoiding chattering effects on sliding surfaces, producing continuous control actions and presenting a reduced computational burden. The control performance is analyzed through representative simulations.

Key Words: Autonomous Surface Vessels, Underactuated Systems, High Order Sliding Mode, Path Following Control

I. Introduction

Nowadays there exist different kinds of devices capable of studying the coastal marine environment characterized by strong and complex links between species and the chemical and physical processes taking place into it. Among all the possible platforms, Autonomous Surface Vessels (ASV) present many advantages respect to other alternatives. Some of them are: simpler and cheaper energy supply, versatility respect to propulsion alternatives, the possibility of more straightforward data communications, larger autonomy, lower construction costs, higher transit speeds, etc. Its main drawback is that they are limited to make near-surface observations.

Considered as single planar rigid bodies ASVs possess three degrees of freedom constituting an underactuated mechanical systems described by complex dynamical models [1][2]. Set-point[3], trajectory tracking [4], and path following [5] control research for autonomous underactuated vessels have received great attention during the last two decades. The main control proposals have traditionally been based on feedback linearization and backstepping methods, however other approaches using passivity, direct Lyapunov, sliding mode and model predictive techniques have also been reported in the specialized literature. A complete review about the advances in this field can be found in the article by Ashrafiuon et al. [2].

This work presents the path following control design for an ASV actuated through two independent propellers. The control objective is to track a predefined geometric path in an environment characterized by the existence of currents and waves. Besides these environmental features, the control design must also overcome the inherent system complexity whose dynamic behavior can be described through a multi-input nonlinear and underactuated model with uncertain parameters. The success of the proposed control is mainly based on the generation of adequate references that ensure the convergence towards the

Manuscript received September 10, 2012.
The author is with LEICI-Facultad de Ingenieria, Universidad Nacional de La Plata and CONICET, C.C 91, C.P 1900, La Plata, ARGENTINA. Email: fval@ing.unlp.edu.ar
This work was supported by the Universidad Nacional de La Plata, CONICET and ANPCyT

desired trajectory. This task is carried-out by a set of guidance laws designed through a standard Lyapunov methodology that, in case of necessity, also allows prioritizing the geometric tracking task fading the trajectory temporal requirements. The control design is approached using second order sliding mode (SOSM) techniques based on the *Super-Twisting* algorithm (STwA) which results very appropriate to produce simple controllers with some features specially attractive in the present case. Some of them are the inherent robustness of the resultant controllers, the chattering free sliding mode behavior, the continuous control signals synthesized by the controllers, the finite and bounded reaching time, their reduced computational cost, etc. [6] [7] [8][9] [10].

II. System Model

Usually, autonomous water vehicles are mathematically described using two reference frames, one fixed to the earth (NED or N-frame) and the other attached to the vessel's centre of buoyancy (B-frame). Thus, in the three dimensional ocean space, the vessel motion can be expressed through a set of six kinetic equations and six kinematic equations relating the vessels position and attitude coordinates and their time derivatives. These kinetic and kinematic equations are respectively referred to the N-frame and the B-frame.

Considering the specific configuration of the ASV described and the mentioned operational constraint, the general dynamic representation of water vessels [11] can be simplified and reduced to a sixth-order model. Thus, the ASV's motion can be appropriately described by [1]:

$$\begin{aligned} \dot{x} &= v_x\, cos(\varphi) - v_y\, sin(\varphi) + \vartheta_x \\ \dot{y} &= v_x\, sin(\varphi) + v_y\, cos(\varphi) + \vartheta_y \\ \dot{\varphi} &= \omega \\ \dot{v}_x &= \left(m_y\, v_y\, \omega - d_x\, v_x^{\alpha_x} + u_1 + \xi_x\right)/m_x \\ \dot{v}_y &= \left(-m_x\, v_x\, \omega - d_y\, sign(v_y)\, |v_y|^{\alpha_y} + \xi_y\right)/m_y \\ \dot{\omega} &= \left(m_d\, v_x\, v_y - d_\omega\, sign(\omega)\, |\omega|^{\alpha_\omega} + u_2 + \xi_\omega\right)/I_\omega \end{aligned} \tag{1}$$

where x, y and φ are the position/attitude coordinates in the NED frame and v_x, v_y and ω are the vessel velocities in the B-frame. On the other hand the parameters m_x, m_y and $m_d = m_y - m_x > 0$ are elements of the called mass matrix while d_x, d_y and I_ω correspond to elements of the damping matrix. It is important to note that this model only considers forward vessel motion ($v_x > 0$). Reverse motion can be quite different because it involves another set of parameters [1].

It should be stressed that the ASV nonlinear dynamic model (1) can be classified as underactuated, presenting only two control variables denoted as u_1 and u_2. These control inputs correspond to the global propeller force and the torque, which are related to the individual propeller's forces f_1 and f_2 through the expressions $u_1 = f_1 + f_2$ and $u_2 = (f_2 - f_1)B/2$, where B is the distance between the propeller's axes. On the other hand, the considered dynamic model also includes the action of perturbations through different variables that represent marine currents (ϑ_x and ϑ_y) and forces produced by waves (ξ_x, ξ_y and ξ_ω).

III. Control Design

The proposed control objective for this particular ASV is to closely track a predefined geometric path on the water surface, considering an environment characterized by the existence of currents and waves. Besides the perturbations action, the control design must also overcome the system complexity whose dynamic behavior is described through the multi-input nonlinear and underactuated model with uncertain parameters (1).

To successfully reach the proposed objective, the control design is faced-out using SOSM and in particular the STwA. This technique has proved to be specially appropriate to cope with nonlinear systems, presenting robust features with respect to system parameter uncertainties and external disturbances [6][12]. On the other hand, this approach allows to mitigate the chattering effect inherent to traditional sliding mode implementations and produce ideally continuous control signals, reducing the mechanical stress on the propellers and therefore on the whole system [7]. The use of the STwA is particularly attractive because its design only needs the nominal system model information and a general knowledge of uncertainties and perturbations acting on it. Besides, the controllers obtained present a reduced on-line computation only based on the sliding variable measurement.

The references used by the sliding controllers are produced by a set of guidance laws designed through the standard Lyapunov methodology. These guidance references are essential to ensure the vessel convergence to the desired path. The mentioned laws are designed to be, in case of necessity, capable to prioritize the geometric tracking task fading the trajectory temporal requirements [13].

3.1. References Generation. A Lyapunov Approach

Lets consider two hypothetical particles on the surface water plane, p_d and $p_p(\varpi)$, respectively characterized in position and speed with respect to the N-frame by the vectors $\mathbf{p}_d = [x_d, y_d]^T$, $\mathbf{p}_p = [x_p(\varpi), y_p(\varpi)]^T$, $\dot{\mathbf{p}}_d = [\dot{x}_d, \dot{y}_d]^T$ and $\dot{\mathbf{p}}_p = [\dot{x}_p(\varpi), \dot{y}_p(\varpi)]^T$. Considering that $p_p(\varpi)$ belongs to a parameterized geometric locus representing the desired path, the objective is to determine the speed ($U_d = \|\dot{p}_d\|$) and direction ($\chi_d = atan(\dot{y}/\dot{x})$) that p_d must follow to reach and track the $p_p(\varpi)$ movements. It must be highlighted that the use of a time dependant parametrization in the desired path expression allows postponing strict time constraints prioritizing, if it were necessary, the geometric tracking task.

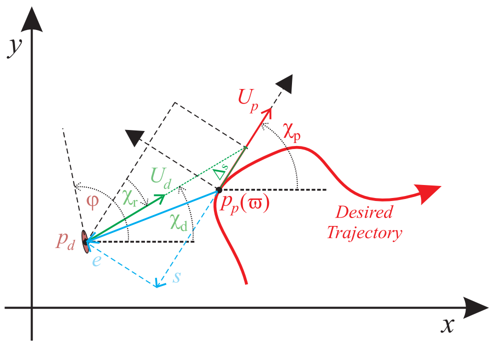

Fig. 1. Guidance scheme

To determine the speed and orientation references for p_d, it is necessary to define its positional error with respect to the instantaneous path particle position. With this purpose, it is useful to define a new reference frame (P-frame), attached to $p_p(\varpi)$ and oriented along the geometric derivative of the desired path in $p_p(\varpi)$, i.e. according to the angle (see Fig.1) [13]:

$$\chi_p = atan\left(\frac{\frac{dy_p(\varpi)}{d\varpi}\frac{d\varpi}{dt}}{\frac{dx_p(\varpi)}{d\varpi}\frac{d\varpi}{dt}}\right) = atan\left(\frac{y'_p(\varpi)}{x'_p(\varpi)}\right) \qquad (2)$$

Considering this definition it is straightforward to determine the transformation matrix from the P-frame to the N-frame. That is:

$$\mathbf{R_p} = \begin{bmatrix} cos(\chi_p) & -sin(\chi_p) \\ sin(\chi_p) & cos(\chi_p) \end{bmatrix} \qquad (3)$$

This rotation matrix maintains the vector magnitudes and therefore it fulfils $\mathbf{R}_p^{-1} = \mathbf{R}_p^T$.

In the P-frame, the position error of p_d is composed by the along-track error, s, and the cross-track error, e. They can be mathematically expressed as:

$$\boldsymbol{\varepsilon} = [s, e]^T = \mathbf{R}_p^T \left(\mathbf{p}_d - \mathbf{p}_p(\varpi)\right) \qquad (4)$$

Then, defining a typical positive definite Lyapunov function in terms of the error ε as:

$$V_\varepsilon = \frac{1}{2}\,\boldsymbol{\varepsilon}\,\boldsymbol{\varepsilon}^T \qquad (5)$$

its time derivative can be written as:

$$\dot{V}_\varepsilon = \boldsymbol{\varepsilon}^T\dot{\boldsymbol{\varepsilon}} = \boldsymbol{\varepsilon}^T(\dot{\mathbf{R}}_p^T(\mathbf{p}_d - \mathbf{p}_p) + \mathbf{R}_p^T(\dot{\mathbf{p}}_d - \dot{\mathbf{p}}_p)) \qquad (6)$$

Next, considering that $\dot{\mathbf{R}}_p$ can be expressed as:

$$\dot{\mathbf{R}}_p = \begin{bmatrix} -\dot{\chi}_p\, sin(\chi_p) & -\dot{\chi}_p\, cos(\chi_p) \\ \dot{\chi}_p\, cos(\chi_p) & -\dot{\chi}_p\, sin(\chi_p) \end{bmatrix} =$$

$$= \underbrace{\begin{bmatrix} cos(\chi_p) & -sin(\chi_p) \\ sin(\chi_p) & cos(\chi_p) \end{bmatrix}}_{\mathbf{R}_p} \underbrace{\begin{bmatrix} 0 & -\dot{\chi}_p \\ \dot{\chi}_p & 0 \end{bmatrix}}_{\mathbf{S}_p} \qquad (7)$$

equation (6) can be rewritten as:

$$\dot{V}_\varepsilon = s(U_d\, cos(\chi_d - \chi_p) - U_p) + eU_d\, sin(\chi_d - \chi_p) \qquad (8)$$

where the particles velocities have been replaced according to:

$$\dot{\mathbf{p}}_p = \mathbf{R}_p\, \mathbf{v}_p = \mathbf{R}_p \begin{bmatrix} U_p \\ 0 \end{bmatrix} \qquad (9)$$

$$\dot{\mathbf{p}}_d = \mathbf{R}_d\, \mathbf{v}_d = \mathbf{R}_d \begin{bmatrix} U_d \\ 0 \end{bmatrix} \qquad (10)$$

It should be noted that the presence of the rotation matrix $\mathbf{R}_d$ in (10), implies the use of another reference frame attached to p_d and aligned with the desired speed vector, i.e involving the angle χ_d (see Fig.1). This matrix allows transforming this vector to the common N-frame.

Watching expression (8), a possible choice for the path particle speed could be:

$$U_p = U_d\, cos(\chi_d - \chi_p) + \gamma s \qquad (11)$$

being $\gamma > 0$ an arbitrary constant associated to the convergence speed of s. On the other hand, from Fig.1 it is straightforward to see that:

$$\chi_r = \chi_d - \chi_p = -atan\left(\frac{e}{\Delta_s - s}\right) \qquad (12)$$

where Δ_s is usually called lookahead distance. The expression proposed for this time-varying variable is:

$$\Delta_s = \eta e^{-\|\varepsilon\|_2/K} \qquad (13)$$

being η and K arbitrary positive constants used to synthesize the shape of Δ_s. It should be stressed that for large errors this lookahead distance vanishes, while for small position errors it tends to η, which is coherent with a general navigation criterion. Then, considering that

$$sin(\chi_r) = \frac{-e}{\sqrt{e^2 + (\Delta_s - s)^2}} \tag{14}$$

expression (8) can be rewritten as:

$$\dot{V}_\varepsilon = -\gamma\, s^2 - U_d \frac{e^2}{\sqrt{e^2 + (\Delta_s - s)^2}} \tag{15}$$

Therefore, choosing U_d as:

$$U_d = \mu\, \sqrt{e^2 + (\Delta_s - s)^2} \tag{16}$$

with $\mu > 0$, conduce to obtain a negative definite expression for the first time derivative of the Lyapunov function:

$$\dot{V}_\varepsilon = -\gamma\, s^2 - \mu\, e^2 < 0 \tag{17}$$

which means that governing the movements of the particles p_d and $p_p(\varpi)$ according to (11), (12) and (16) determines the uniform global and exponential convergence of the positional error ε to zero.

At this point it should be noted that p_p was considered parameterized by the variable ϖ. Thus, from (11) it is straightforward to write:

$$\|\mathbf{v}_p\|_2 = U_p = \|\mathbf{R}_p^T\, \dot{\mathbf{p}}_p\|_2 = \sqrt{x'^2_p + y'^2_p}\ \dot{\varpi} \tag{18}$$

from where the equation to dynamically refresh this parameter can be written as:

$$\dot{\varpi} = \frac{U_p}{\sqrt{x'^2_p + y'^2_p}} = \frac{U_d\, cos(\chi_r) + \gamma s}{\sqrt{x'^2_p + y'^2_p}} \tag{19}$$

Finally, according to Fig.1 it is straightforward to determine that the wanted guidance laws can be expressed by:

$$v_x^* = \mu \sqrt{e^2 + (\Delta_s - s)^2}\, cos(\varphi - \chi_d) \tag{20}$$

$$\varphi^* = \chi_d = \chi_p + \chi_r \tag{21}$$

3.2. SOSM-STwA Control Design

The control objective considered in this work is to reach and closely follow a pre-specified trajectory in an environment perturbed by currents and waves. Taking into account that the system presents only two control actions, a pair of sliding variables representing the control objectives, s_1 and s_2 must be defined. Then, having in mind the necessary relative degree condition for the sliding vector $\boldsymbol{S} = [s_1 \;\; s_2]^T$, the following surfaces are proposed:

$$s_1(\boldsymbol{x}, t) = v_x - v_x^*(t) \tag{22}$$

$$s_2(\boldsymbol{x}, t) = \varphi - \varphi^*(t) + \rho(\dot{\varphi} - \dot{\varphi}^*(t)) \tag{23}$$

where $\rho > 0$ and v_x^*, φ^* are the references determined by the guidance laws and presented in the previous subsection. It should be noted that the second sliding variable is in fact a Hurwitz dynamic surface involving a time derivative term added to fulfill the necessary vectorial relative degree condition (VRD=$[1,\ 1]$).

From (22) and (23) and rewriting the dynamic system model (1) under the structure:

$$\dot{\boldsymbol{x}} = \underbrace{\boldsymbol{F}(\boldsymbol{x}) + \Delta\boldsymbol{F}(\boldsymbol{x}, t) + \boldsymbol{\xi}(t)}_{\widetilde{\boldsymbol{F}}} + \boldsymbol{G}\, \boldsymbol{u} \tag{24}$$

where $\boldsymbol{x} \in \Re^n$ is the states vector and $\boldsymbol{u} \in \Re^m$ is the control vector, $\boldsymbol{F}$ represents the nominal drift vector, $\Delta\boldsymbol{F}(\boldsymbol{x}, t)$ is an explicitly time dependant drift vector originated in unknown slow temporal parameter variations, $\boldsymbol{\xi}(t)$ represents the influence of bounded and continuous external perturbations and finally, $\boldsymbol{G} = [\boldsymbol{g}_1\, \boldsymbol{g}_2]$ is the system control matrix, it is straightforward to obtain the expression of $\dot{\boldsymbol{S}}$ as:

$$\dot{\boldsymbol{S}} = \begin{bmatrix} L_{\widetilde{\boldsymbol{F}}} s_1 + \frac{\partial s_1}{\partial t} \\ L_{\widetilde{\boldsymbol{F}}} s_2 + \frac{\partial s_2}{\partial t} \end{bmatrix} + \begin{bmatrix} L_{\boldsymbol{g}_1} s_1 & 0 \\ 0 & L_{\boldsymbol{g}_2} s_2 \end{bmatrix} \boldsymbol{u} \tag{25}$$

where:

$$L_{\widetilde{\boldsymbol{F}}} s_1 + \frac{\partial s_1}{\partial t} = \frac{m_y v_y \omega - d_x v_x^{\alpha_x} + \xi_x}{m_x} - \dot{v}_x^*$$

$$L_{\widetilde{\boldsymbol{F}}} s_2 + \frac{\partial s_2}{\partial t} = \omega - \dot{\varphi}^* +$$
$$+ \rho \left(\frac{m_d v_x v_y - d_\omega\, |\omega|^{\alpha_\omega}\, sign(\omega) + \xi_\omega}{I_\omega} - \ddot{\varphi}^* \right)$$

$$L_{\boldsymbol{g}_1} s_1 = 1/m_x \quad L_{\boldsymbol{g}_2} s_2 = -\rho/I_\omega$$

In these last expressions the time derivatives of the slow time varying model parameters have been considered null. On the other hand, it is important to note that the proposed sliding variables produce in (25) a diagonal control matrix. This feature simplifies the control design task because there is an unique possible control assignment implicitly imposed by the system structure [14], being the force u_1 and the torque u_2 the only control actions to respectively drive the system towards

$s_1 = 0$ and $s_2 = 0$. Thus, the control design task can be tackled considering two uncoupled SOSM SISO controllers . With this purpose, from (25), the second time derivative expression of $\ddot{\mathbf{S}}$ can be written as:

$$\ddot{\mathbf{S}} = \begin{bmatrix} L^2_{\widetilde{\mathbf{F}}} s_1 + \frac{\partial L_{\widetilde{\mathbf{F}}} s_1}{\partial t} \\ L^2_{\widetilde{\mathbf{F}}} s_2 + \frac{\partial L_{\widetilde{\mathbf{F}}} s_2}{\partial t} \end{bmatrix} + \\ + \begin{bmatrix} L_{\boldsymbol{g}_1} L_{\widetilde{\mathbf{F}}} s_1 & L_{\boldsymbol{g}_2} L_{\widetilde{\mathbf{F}}} s_1 \\ L_{\boldsymbol{g}_1} L_{\widetilde{\mathbf{F}}} s_2 & L_{\boldsymbol{g}_2} L_{\widetilde{\mathbf{F}}} s_2 \end{bmatrix} \begin{bmatrix} u_1 \\ u_2 \end{bmatrix} + \\ + \begin{bmatrix} L_{\boldsymbol{g}_1} s_1 & 0 \\ 0 & L_{\boldsymbol{g}_2} s_2 \end{bmatrix} \begin{bmatrix} \dot{u}_1 \\ \dot{u}_2 \end{bmatrix} \quad (26)$$

where $\boldsymbol{g}_k$ is the k column of the matrix $\boldsymbol{G}$. Given that all the expressions involved in (26) correspond to continuous bounded functions, considering the operational limits of the system and the general features of the disturbances influencing on it, there can be found two sets of constants $\underline{K}_{s_i}$, $\overline{K}_{s_i}$, C_{s_i}, U_{M_i} and q_{s_i} with $i = 1, 2$ that fulfill the inequalities:

$$0 < q_{s_i} < 1 \quad (27)$$

$$0 < \underline{K}_{s_i} < L_{\boldsymbol{g}_i} s_i < \overline{K}_{s_i} \quad (28)$$

$$\left| L^2_{\widetilde{\mathbf{F}}} s_i + \frac{\partial L_{\widetilde{\mathbf{F}}} s_i}{\partial t} \right| + \sum_{k=1}^{2} \left| L_{\boldsymbol{g}_k} L_{\widetilde{\mathbf{F}}} s_i \right| U_{M_k} \leq C_{s_i} \quad (29)$$

$$\left| \frac{L_{\widetilde{\mathbf{F}}} s_i + \frac{\partial s_i}{\partial t}}{L_{\boldsymbol{g}_i} s_i} \right| < q_{s_i} U_{M_i} \quad (30)$$

Taking into account (27)-(30), it is straightforward to find that each second time derivative $\ddot{s}_i$ of (26) belongs to the differential inclusion:

$$\ddot{s}_i \in [-C_{s_i},\ C_{s_i}] + \left[\underline{K}_{s_i},\ \overline{K}_{s_i}\right] \nu_i \quad (31)$$

where ν_i is the corresponding control time derivative. This differential inclusion contains all the possible system dynamics for any perturbations and parameter variation (inside the considered limits) acting on the system in its whole operational range. Then, according to the STwA, if the parameters α_{s_i} and γ_{s_i} are chosen conserving the inequalities:

$$\underline{K}_{s_i} \alpha_{s_i} > C_{s_i} \quad (32)$$

$$\gamma_{s_i} > \sqrt{\frac{2}{\underline{K}_{s_i} \alpha_{s_i} - C_{s_i}} \frac{\overline{K}_{s_i} (\underline{K}_{s_i} \alpha_{s_i} - C_{s_i})(1 - q_{s_i})}{\underline{K}^2_{s_i} (1 + q_{s_i})}} \quad (33)$$

the SOSM-STwA controllers:

$$u_i = -\gamma_{s_i} |s_i|^{1/2} sign(s_i) + \nu_i \quad (34)$$
$$\dot{\nu}_i = \begin{cases} -u_i & |u_i| > U_{M_i} \\ -\alpha_{s_i} sign(s_i) & |u_i| \leq U_{M_i} \end{cases}$$

provide for the finite time system convergence of any uncertain and perturbed system in (31) to the manifold $s_i = \dot{s}_i = 0 \;\; i = 1, 2$, being the reaching time a locally bounded function of the initial conditions [8]. This means that the resultant controllers are robust against the set of perturbations and parameter variations preserving (31). Once the system is in sliding mode, the motion is characterized by chattering absence.

In order to choose the controller parameters α_i, γ_i and U_{Mi} for $i = 1, 2$, it is necessary to explicitly obtain the analytic expressions involved in (26). Next, after long but straightforward algebraic manipulations bounds (27)-(30) are obtained regarding the operational limits and the maximum levels of perturbations and unmodeled dynamics acting on the system. After carrying-out this first analytic procedure, the parameters of the controller for each sliding surface can be selected according to expressions (32)-(33) to obtain a good reaching performance. This last tuning phase is commonly realized complementing analytic and simulation tools [15][16].

IV. Simulation Results

Exhaustive simulations were carried out to assess the performance of the proposed control. To develop these simulations, the vessel parameters and their uncertainty ranges were taken from [1]:

$$\begin{array}{rr} m_x = 1.956 \pm 0.019\ Kg & m_y = 2.405 \pm 0.117\ Kg \\ I_\omega = 0.403 \pm 0.0068\ Kg.m & d_x = 2.436 \pm 0.023 \\ d_y = 12.992 \pm 0.297 & d_\omega = 0.0564 \pm 0.00085 \\ \alpha_x = 1.510 \pm 0.0075 & \alpha_y = 1.747 \pm 0.013 \\ \alpha_\omega = 1.592 \pm 0.0285 & B = 0.07\ m \\ H = 0.15\ m & D = 0.20\ m \end{array}$$

The simulation tests were performed using as desired trajectory a closed elipsoidal path starting clockwise from the point $[1, 4.5, \pi/2]$. The vessel was initially considered at rest being its initial position $[x_0, y_0, \varphi_0] = [0, 0, \pi/4]$. Disturbances due to marine currents and waves have been included in the simulation tests. In particular the former was considered acting with a speed of about the 10% of the maximum vessel speed and a direction determined by an angle of $\delta_c = \pi/4$. The action of waves was characterized by the time profile depicted in Fig.2 with a propagation angle of 0 rad. This force is represented in a percentage scale using the maximum force produced by the boat propellers as reference. Its effect on the fourth, fifth and sixth components of (1) depends on the vessel orientation, reaching in the worst case the 15% level. On the other hand, model inaccuracies have been considered using a set of parameters randomly chosen within the ranges previously defined.

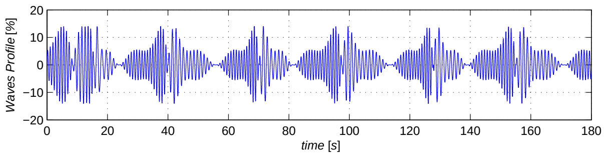

Fig. 2. Waves train profile

Taking into account these specifications and the ASV operational range, the following controllers parameters were selected according to the process described in the previous section: $\alpha_{s_1} = 11.5$; $\gamma_{s_1} = 4$; $U_{M_{s_1}} = 3$; $\alpha_{s_2} = 18$; $\gamma_{s_2} = 7.5$; $U_{M_{s_2}} = 6$ and $\rho = 1$.

To analyze the controller performance Fig.3 presents in the $x - y$ plane the desired path and the vessel trajectory and Fig.4 the time profiles of errors. To complement theses images, Fig.5 depicts the time evolution of the variables U_d, U_p and ϖ, and Fig.6 shows the sliding variables behavior.

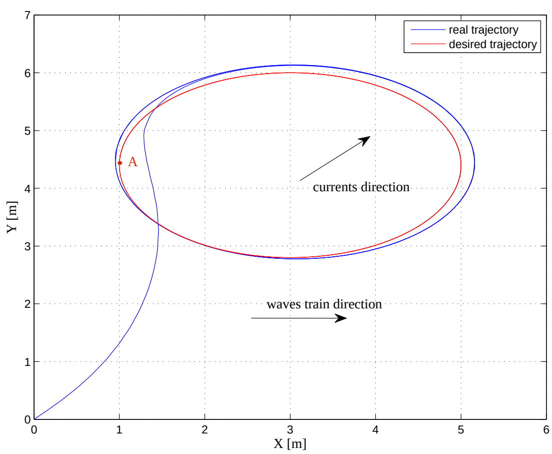

Fig. 3. Vessel trajectory and desired trajectory

As it can be appreciated in Fig.3, the vessel initially describes a free approaching path, looking for the starting trajectory point (A). The shape of this initial reaching path depends on the parameters ρ, μ and γ established in the design stage. Given that the fictitious

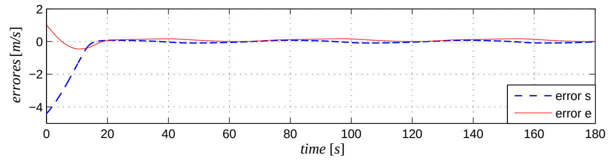

Fig. 4. Positional errors s and e

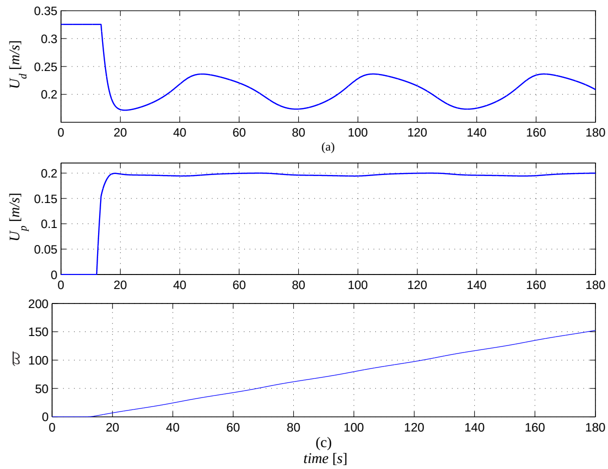

Fig. 5. Guidance variables a) U_d b) U_p c) ϖ

particle p_p starts moving when the vessel is in the neighborhood of point A (approximately at $t = 2.5sec.$ when the error s decreases enough to produce an $U_p > 0$ and therefore $\varpi > 0$ (see Fig.5)) the initial path reaches the desired trajectory beyond that point. After this approximation phase the designed control is able to follow the specified path even in the presence of waves and currents. The magnitude of the position errors observed in Fig.3 are determined by the small scale of the desired trajectory chosen respect to the vessel dimensions. Larger trajectories present similar absolute position errors but not significant relative errors.

Respect to the navigation variables, it should be noted in Fig.5 that U_d initially appears upper saturated to prevent a reference greater than the maximum vessel speed. On the other hand U_p and therefore ϖ are zero lower saturated to avoid inversions in the trajectory direction. It is also interesting to observe that after the first $20sec.$ U_p and U_d present oscillatory profiles. This is produced by the chosen trajectory shape. On regions where the desired path presents a high curvature the propellers must be mainly used to change the vessel direction and not to generate a forward force and viceversa.

The control performance can be analyzed through the sliding variables behavior. As it can be seen

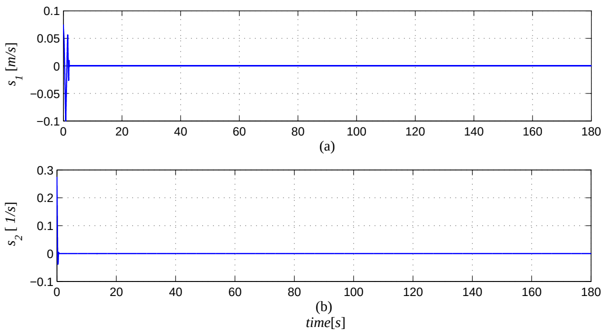

Fig. 6. Sliding surfaces a) s_1; b) s_2

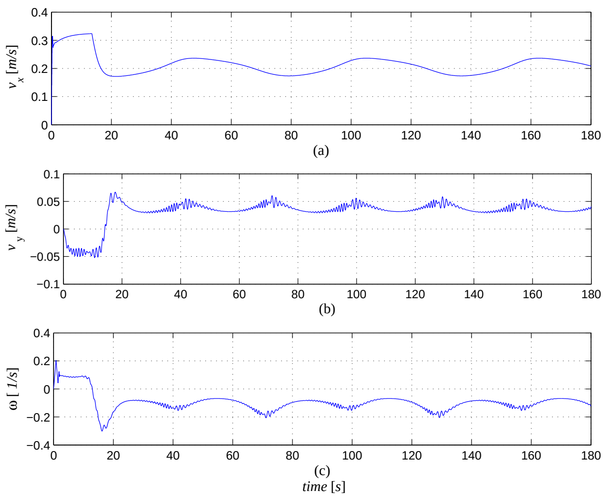

Fig. 7. System states a) v_x and v_y; b) ω

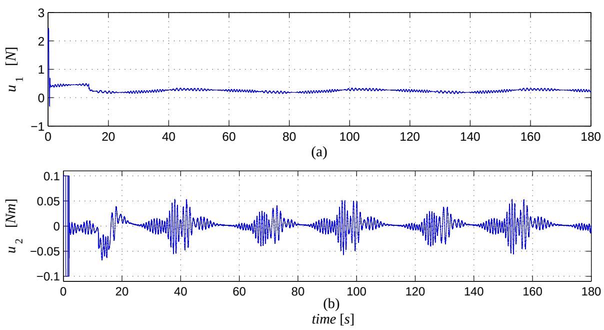

Fig. 8. Control components

in Fig.6, after convergence the control successfully deals with the complex nature of the reaching and tracking task (even in the presence of disturbances and model inaccuracies), taking the system to operate on the designed sliding surfaces. To complete the analysis, Figs.7 and 8 present the time profiles of the system states and the control variables respectively. In particular, it is important to stress the smoothness of the control variables u_1 and u_2, determined by the use of SOSM control techniques. This chattering-free characteristic is specially attractive because it reduces the mechanical stress on the propellers extending their operative life .

Finally, the phase portraits corresponding to the system reaching phase to the sliding surfaces are separately depicted in Fig.9. These plots show the typical form that systems controlled by STwA algorithms draw during convergence.

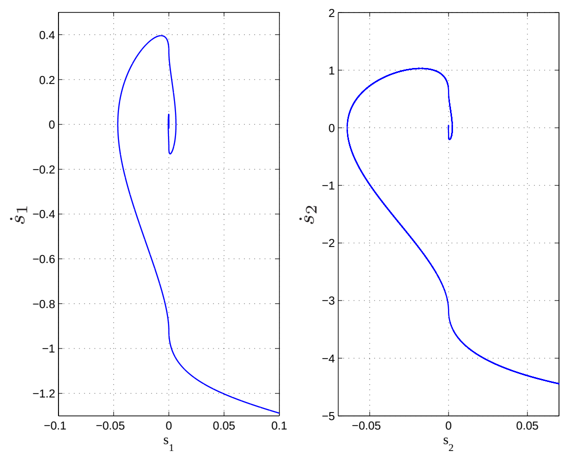

Fig. 9. Surfaces reaching phase portraits a) $\dot{s}_1 - s_1$; b) $\dot{s}_2 - s_2$

V. Conclusions

This paper presents a successful path following control design applied to an ASV described by an uncertain nonlinear dynamic model and considering an environment characterized by the presence of continuous bounded perturbations (currents and waves). The control scheme is approached through a MIMO HOSM controller whose sliding surfaces are designed to fulfil the proposed control objective and simultaneously obtain the necessary vectorial relative degree. The references used by these sliding surfaces are generated on-line by a set of guidance laws synthesized through Lyapunov techniques. This technique permits to incorporate a geometric locus continuously parameterized by a time dependant scalar variable, which facilitates to relax the path following time requirements prioritizing, if it were necessary, the geometric tracking task. This control scheme allows closely following the desired path ensuring the uniform, global and exponential convergence toward it. The controlled closed-loop system shows a very good performance with additional attractive features like a chattering-free behavior, a finite reaching time phase and excellent robustness properties against external disturbances and unmodeled dynamics (parameters uncertainty). Besides, the smoothness of the control variables determined by the use of SOSM-STwA this approach is specially attractive because it reduces the mechanical stress on the propellers, extending their utility life. The implementation of the proposed controller does not require more computational cost than the necessary to implement a control scheme based on traditional PIDs. The presented results are easily extensible to other water vehicle topologies used for path following applications.

REFERENCES

1. H. Ashrafiuon, K. R. Muske, L. C. McNinch, and R. A. Soltan, *Sliding-mode tracking control of surface vessels*, IEEE Trans. Idust. Elect., vol. 55(11), pp. 4004-4012, nov 2008. DOI:10.1109/TIE.2008.2005933
2. H. Ashrafiuon, K. R. Muske, and L. C. McNinch, *Review of nonlinear tracking and setpoint control approaches for autonomous underactated marine vehicles*, in 2010 American Control Conference, Baltimore,MD, USA, pp. 5203-5211, (2010).
3. W. Dong and Y. Guo, *Global Time Varying Stabilization of Underactuated Surface Vessels*, IEEE Trans. A. Control, vol.50(6), pp.859-864, 2005. DOI:10.1109/TAC.2005.849248
4. G. Bartolini and A. Pisano, *Black Box Position and Attitude Tracking for underwater vehicles by second-order Sliding Mode Technique*, Int. J. of Robust and Nonlinear Control, vol.20(14), pp.1594-1609, 2010. DOI:10.1002/rnc.1532
5. Z. Li, J. Sun and S. Oh, *Path Following for Marine Surface Vessels with Rudder and Roll Constraints*, in 2009 American Control Conference, St. Louis, Missouri, USA, pp. 3611-3619, (2009)
6. G. Bartolini, A. Pisano, E. Punta, and E. Usai, *A survey of applications of second order sliding mode control to mechanical systems*, Int. J. of Control, vol. 76(9/10), pp. 875-892, (2003). DOI:10.1080/0020717031000099010
7. L. Fridman and A. Levant, *Sliding Mode Control in Engineering*. Marcel Dekker, Inc., (2002), ch. 3: Higher Order Sliding Modes, pp. 53-101. DOI:10.1201/9780203910856.ch3
8. A. Levant, *Introduction to high-order sliding modes*, Available On Line: http://www.tau.ac.il/ levant/hosm2002.pdf, (2003).
9. M.K.Khan, K.B. Goh and S.K. Spurgeon, *Second Order Sliding Mode Control of a Diesel Engine*, Asian Journal of Control, vol.5(4), pp.614-619, (2003). DOI:10.1111/j.1934-6093.2003.tb00177.x
10. A. Sabanovic, L. Fridman, S.K. Spurgeon *Variable Structure Systems: From Principles to Implementation* IET, (2004).
11. T. H. Fossen, *Marine Control Systems. Guidance, Navigation and Control of Ships, Rigs and Underwater Vehicles*. Marine Cybernetics AS., 2002.
12. M. Tanelli and A. Ferrara, *Switched Second Order Sliding Mode Control with Partial Information: Theory and Application*, Asian J. of Control, vol. 15(1), pp. 20-30, (2012). DOI:10.1002/asj.540
13. M. Breivik and T. Fossen, *Principles of guidance-based path following in 2D and 3D*, in IEEE Conference on Decision and Control, CDC05, pp. 627-634, (2005). DOI:10.1109/CDC.2005.1582226
14. A. Levant, *Mimo 2-sliding control design*, European Control Conf., Cambridge, UK, 2003.
15. C. Evangelista, P. Puleston, F. Valenciaga, and A. Davila, *Variable gains super-twisting control for wind energy conversion optimization*, 11th International Workshop on Variable Structure Systems, Mexico City, (2010).
16. G. Bartolini, A. Ferrara, A. Levant, and E. Usai, *Variable Structure Systems, Sliding Modes and Nonlinear Control, Chapter 17: Second Order Sliding Mode Controllers*. Springer, (1999).

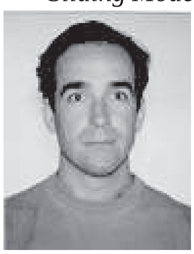

F.Valenciaga received the B.S.E.E. degree and the Ph.D. degrees in 1993 and 2001, respectively, from National University of La Plata(UNLP), La Plata, Argentina. Currently, he is Assistant Professor of automatic control in the Electrical Engineering Department at UNLP. His primary area of interest is automatic control systems.